

# Properties of compressible elastica from relativistic analogy

Oz Oshri\*

Raymond & Beverly Sackler School of Physics & Astronomy, Tel Aviv University, Tel Aviv 6997801, Israel

Haim Diamant†

Raymond & Beverly Sackler School of Chemistry, Tel Aviv University, Tel Aviv 6997801, Israel

(Dated: November 14, 2018)

Kirchhoff's kinetic analogy relates the deformation of an incompressible elastic rod to the classical dynamics of rigid body rotation. We extend the analogy to compressible filaments and find that the extension is similar to the introduction of relativistic effects into the dynamical system. The extended analogy reveals a surprising symmetry in the deformations of compressible elastica. In addition, we use known results for the buckling of compressible elastica to derive the explicit solution for the motion of a relativistic nonlinear pendulum. We discuss cases where the extended Kirchhoff analogy may be useful for the study of other soft matter systems.

Analogies to dynamical problems have been used to simplify the physics of various condensed-matter systems, ranging from the deformation of elastic bodies to the order-parameter profile across an interface between co-existing phases. A particularly well known example is Kirchhoff's kinetic analogy [1]. In this theory the three-dimensional (3D) deformation of a slender elastic rod is reduced to the bending deformation of an incompressible curve, representing the mid-axis of the rod. This problem, in turn, is analogous to the dynamics of a rigid body rotating about a fixed point, where the distance along the curve and its local curvature are analogous, respectively, to time and angular velocity. When the filament is confined to a two-dimensional (2D) plane (the celebrated Euler elastica [2]), the equation of equilibrium coincides with the equation of motion of a physical pendulum [1, 19].

In the examples above the elastic system was reduced to an indefinitely thin, incompressible body, whose equilibrium shape follows the trajectory of a classical dynamical system. In the present work we show that relaxing the incompressibility constraint introduces terms akin to relativistic corrections to classical dynamics. Within this analogy, the compression modulus,  $Y$ , plays the role of the relativistic particle's rest mass, and the bendability parameter  $(Y/B)^{1/2} \equiv h^{-1}$ , where  $B$  is the bending modulus, is analogous to the speed of light. The limit of an incompressible rod ( $h \rightarrow 0$ ) corresponds to the nonrelativistic limit.

Despite the relevance to real systems, including compressible fluid membranes [4], there have not been many studies of compressible elastica (see [5] and references therein). Following these works, we consider the 2D deformation of a compressible filament, represented by a planar curve of relaxed length  $L$ . The same model applies to thin elastic sheets, as well as fluid membranes [6], provided that they are deformed along a single direction. The deformation away from the flat, stress-free

state is parametrized by the angle  $\phi(s)$  and compressive strain  $\gamma(s)$ , as functions of the relaxed arclength  $s$  along the curve,  $s \in [0, L]$ ; see Fig. 1(a). We denote the compressed arclength by  $\hat{s}$ , such that  $\gamma = d\hat{s}/ds$  and the total deformed length is  $\hat{L} = \int_0^{\hat{L}} d\hat{s} = \int_0^L \gamma(s) ds$ .

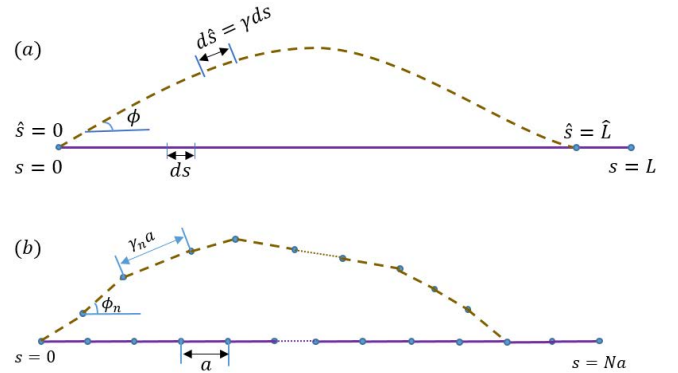


FIG. 1. (a) Deformed and undeformed configurations. The straight line (solid, purple) represents a relaxed rod of initial length  $L$ , and the curved line (dashed, gold) represents a deformed rod of total length  $\hat{L}$ . Their arclength parameters are  $s$  and  $\hat{s}$  respectively. The local in-plane and out-of-plane deformations are respectively accounted for by the compression field  $\gamma = d\hat{s}/ds$  and the angle  $\phi(s)$ . (b) An illustration of the discrete model. The initial, zero-energy configuration (solid, purple) consists of  $N$  rigid bonds of rest length  $a$  and zero joint angles. A higher-energy state (dashed, gold) is obtained by compression of each bond,  $a \rightarrow \gamma_n a$ , and/or a change of each joint angle,  $\phi_n$ . The continuous limit of this model yields the picture presented in panel (a).

To obtain the energy functional which keeps the bending and compression contributions independent, it is instructive to start from a discrete model (see Fig. 1(b)). Consider a chain of  $N$  jointly connected compressible rigid bonds of rest length  $a$ . The chain's configuration is parametrized by a set of bond strains  $\gamma_n$  ( $1 \leq n \leq N$ ) and a set of joint angles  $\phi_n$  ( $1 \leq n \leq N-1$ ). The

\* ozzoshri@tau.ac.il

† hdiamant@tau.ac.il

energy of a given configuration has a compression contribution,  $E_c = (Y/2a) \sum_{n=1}^N (\gamma_n a - a)^2$ , and a bending contribution,  $E_b = (B/2a) \sum_{n=1}^{N-1} (\phi_{n+1} - \phi_n)^2$ . For the sake of the analogy we add a potential energy of the form,  $E_p = a \sum_{n=1}^N \gamma_n V(\phi_n)$ , where  $V(\phi)$  is an angle-dependent potential. This choice of potential energy is not artificial. For example, if we include an external work on the chain, coupling the force  $P$  exerted on the boundaries with the chain's projected length, we have  $E_p = Pa \sum_{n=1}^N \gamma_n \cos \phi_n$ , i.e.  $V(\phi) = P \cos \phi$ . We now take the continuum limit,  $N \rightarrow \infty$  and  $a \rightarrow 0$  such that  $Na \rightarrow L$  and  $na \rightarrow s$ , getting,

$$E[\phi(s), \gamma(s)] = E_b + E_c + E_p \\ = \int_0^L ds \left[ \frac{B}{2} \left( \frac{d\phi}{ds} \right)^2 + \frac{Y}{2} (\gamma - 1)^2 + \gamma V(\phi) \right]. \quad (1)$$

To obtain the equations of equilibrium for the filament one should minimize  $E$  with respect to  $\gamma(s)$  and  $\phi(s)$ . This gives the two equations,

$$Y(\gamma - 1) + V = 0, \quad (2)$$

$$B \frac{d^2 \phi}{ds^2} - \gamma \frac{dV}{d\phi} = 0. \quad (3)$$

First integration yields,

$$\mathcal{H} = \frac{B}{2} \left( \frac{d\phi}{ds} \right)^2 - \frac{Y}{2} (\gamma - 1)^2 - \gamma V = \text{const}, \quad (4)$$

which depends on the boundary conditions at  $s = 0, L$ .

The mathematical analogy to relativistic dynamics is revealed once we transform from the relaxed arclength,  $s$ , to the compressed one,  $\hat{s}$ , and redefine the potential as  $\bar{V} = -V$ . Equation (3) then turns into

$$B \frac{d}{d\hat{s}} \left( \gamma \frac{d\phi}{d\hat{s}} \right) + \frac{d\bar{V}}{d\phi} = 0. \quad (5)$$

This equation is analogous to the Euler-Lagrange equation for the one-dimensional motion of a relativistic particle [7], provided that  $\gamma(\hat{s})$  coincides with the Lorentz factor. To obtain  $\gamma$  we use eqn (4) to eliminate  $V$  in eqn (2), and transform to  $\hat{s}$ , which gives,

$$\gamma = \frac{\sqrt{1 + 2\mathcal{H}/Y}}{\sqrt{1 + h^2(d\phi/d\hat{s})^2}}. \quad (6)$$

This expression indeed resembles the Lorentz factor up to the constant prefactor,  $\gamma_0 \equiv \sqrt{1 + 2\mathcal{H}/Y}$ . Absorbing this prefactor in the potential  $\bar{V}$  makes eqn (5) identical to the relativistic one, with the correct Lorentz factor. This completes the analogy. The mapping between the variables and parameters of these two systems is summarized in Table I.

We now use the mapping to identify a new symmetry of compressible elastica. First, recall that the equation of equilibrium of *incompressible* elastica is invariant to

TABLE I. Mapping between the parameters of compressible elastica and relativistic dynamics

Elasticity	Relativity
relaxed arclength <sup>a</sup> , $s$	proper time, $\tau$
compressed arclength, $\hat{s}$	laboratory time, $t$
tangent angle, $\phi$	angle coordinate, $\phi$
curvature, $\kappa = d\phi/d\hat{s}$	angular velocity, $\omega = d\phi/dt$
compression field <sup>a</sup> , $\gamma = d\hat{s}/ds$	Lorentz factor, $\gamma = dt/d\tau$
compression modulus, $Y$	minus the rest energy, $-mc^2$
bending modulus, $B$	moment of inertia, $m\ell^2$
bendability, $h^{-1} = \sqrt{Y/B}$	speed of light, $c$

<sup>a</sup> More accurately, the analogue of  $\tau$  is  $\gamma_0 s$ , where  $\gamma_0$  is a constant prefactor (see text).

the addition of a constant curvature  $\kappa$ , making a flat configuration cylindrical. The kinetic analogue of this symmetry is the Galilean invariance of the equation of motion of a classical free particle to a boost by a constant velocity. We are after the corresponding symmetry for a *compressible* elastic filament. It is natural to try the analogue of a Lorentz boost. To make the connection to a free particle we first remove the potential energy from eqn (5),  $\bar{V}(\phi) = 0$ , and then divide by  $B\gamma_0$ . The resulting equation of elastic equilibrium,

$$\frac{d}{d\hat{s}} \left( \frac{1}{\sqrt{1 + h^2(d\phi/d\hat{s})^2}} \frac{d\phi}{d\hat{s}} \right) = 0, \quad (7)$$

is identical to the equation of motion of a free relativistic particle. With the Lorentz boost in mind, we immediately identify the transformation of coordinates  $(\hat{s}/h, \phi) \rightarrow (\hat{S}/h, \Phi)$ , which leaves eqn (7) unchanged:

$$\begin{pmatrix} \hat{s}/h \\ \phi \end{pmatrix} = \begin{pmatrix} \gamma & -\gamma h \kappa \\ \gamma h \kappa & \gamma \end{pmatrix} \begin{pmatrix} \hat{S}/h \\ \Phi \end{pmatrix}, \quad (8)$$

where  $\kappa = \text{const}$ , and  $\gamma = 1/\sqrt{1 + h^2 \kappa^2}$ . The transformation is a rotation of the material coordinates,  $(\hat{s}/h, \phi)$ , by an angle  $\theta = \sin^{-1}(\gamma h \kappa)$ , turning a flat, relaxed configuration into a cylindrical, compressed one; see Fig. 2. The rotation leaves the line element on the material-coordinates plane unchanged,  $d\hat{s}^2/h^2 + d\phi^2 = d\hat{S}^2/h^2 + d\Phi^2$ . This reparametrization invariance defines a continuous family of solutions to the equation of equilibrium, containing all the cylindrical, compressed configurations of the filament. These configurations satisfy local mechanical equilibrium but differ in their total energy. (Obviously, the flat relaxed configuration always has the lowest energy.) The actual equilibrium configuration for a given problem is selected by boundary conditions. To our knowledge, this symmetry of compressible filaments has not been recognized before.

An important physical distinction should be made, however, between the two sides of the analogy. In the

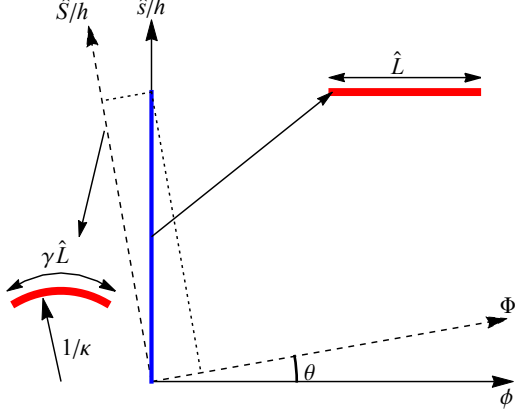


FIG. 2. Rigid rotation of the coordinate system  $(\hat{s}/h, \phi) \rightarrow (\hat{S}/h, \Phi)$  by an angle  $\theta$ . A flat elastic filament of length  $\hat{L}$  is described by the blue line. As viewed from the new frame, the total length is compressed by a factor  $\gamma$ , and the angle coordinate,  $\Phi$ , is linearly changing, resulting in a cylindrical compressed shape of radius  $1/\kappa$  and length  $\gamma\hat{L}$ .

elastic problem there is a unique zero-energy state, and one naturally specifies the length  $L$  and the boundary conditions with respect to that relaxed state; the compressed length  $\hat{L}$  is determined by minimization. By contrast, in relativity there is no preferred reference frame, and the duration of the experiment and the boundary conditions are given in the laboratory frame, not the proper one. This difference leads to the extra prefactor  $\gamma_0$  above. Thanks to this prefactor the elastic strain can be either compressive or dilative, whereas the relativistic Lorentz factor must be dilative.<sup>1</sup> Note that, because of the minus sign in the mapping  $Y \rightarrow -mc^2$ , time dilation corresponds to elastic compression.

Despite the physical difference, by absorbing the factor  $\gamma_0$  in the potential, the two problems become mathematically equivalent. Thus, a known solution in one system can be readily transferred to the other. We shall now use known results for the buckling of compressible elastica to write down an explicit solution to the equation of motion of a relativistic nonlinear pendulum. (A solution to this dynamical system was previously given only in implicit parametric form [11].)

To do so, we should specialize to the potential  $V(\phi) = P \cos \phi$ . Substitution of  $V$  in eqn (2) gives  $\gamma = 1 - (P/Y) \cos \phi$ . These expressions for  $V$  and  $\gamma$  turn eqn (3)

into

$$B \frac{d^2 \phi}{ds^2} + P \sin \phi - \frac{P^2}{Y} \sin \phi \cos \phi = 0, \quad (9)$$

which is the equation of equilibrium for a compressible elastica under a uniaxial force  $P$  [5, 8]. The exact solution to eqn (9) was derived in ref. [5]. For hinged boundary conditions,  $d\phi/ds = 0$  at  $s = 0, L$ , it is given by

$$\phi(s) = 2 \sin^{-1} \left[ q \frac{(1 - (qkh)^2/\gamma_0)^{1/2} \text{cd}(\sqrt{\gamma_0}ks, m)}{[1 - (qkh)^2/\gamma_0 \text{cd}^2(\sqrt{\gamma_0}ks, m)]^{1/2}} \right]. \quad (10)$$

Hereafter we use the conventional symbols for the various elliptic functions,  $\text{cd}, \text{am}, K$  and  $\Pi$ , as defined in ref. [9]. In addition,  $k \equiv \sqrt{P/B}$  is the wavenumber of the buckled *linear* elastica. We have defined three additional parameters which depend on the boundary angle,  $\phi_0 \equiv \phi(s = 0)$ :

$$\begin{aligned} q &\equiv \sin(\phi_0/2) \\ \gamma_0 &= 1 - (kh)^2 \cos \phi_0 \\ m &= q^2 [1 + (qkh)^2] / \gamma_0. \end{aligned} \quad (11)$$

The parameter  $\gamma_0 = \gamma(s = 0)$  gives the boundary strain, which coincides with  $\gamma_0$  as defined above. The actual wavelength (periodicity)  $\lambda$  of the nonlinear buckled elastica is

$$\lambda = 4K(m)/(\sqrt{\gamma_0}k). \quad (12)$$

The total rod length matches a half wavelength,  $L = \lambda/2$ . This expression relates  $\phi_0$  to the force  $P$  and the system parameters via eqn (11). The total deformed length is given by  $\hat{L} = \int_0^L [1 - (kh)^2 \cos \phi] ds$ , yielding,

$$\hat{L}/L = 1 - (kh)^2 \left[ 2(1 - q^2) \frac{\Pi(q^2, m)}{K(m)} - 1 \right]. \quad (13)$$

It is readily shown that the three known solutions for incompressible nonlinear elastica ( $h \rightarrow 0$ ) [1], compressible linear elastica ( $\phi_0 \ll 1$ ) [5], and incompressible linear elastica ( $h \rightarrow 0, \phi_0 \ll 1$ ) [1], are obtained from eqn (10) in the respective limits.

To apply the analogy, we first transform eqn (9) to the deformed arclength  $\hat{s}$  using equations (2), (4) and (6). This leads to

$$\frac{d}{d\hat{s}} \left( \frac{1}{\sqrt{1 + h^2(d\phi/d\hat{s})^2}} \frac{d\phi}{d\hat{s}} \right) + \frac{k^2}{\gamma_0} \sin \phi = 0. \quad (14)$$

Next, substituting

$$\{h^2, k^2/\gamma_0\} \rightarrow \{-\ell^2/c^2, \omega^2\},$$

where  $\omega$  is the natural frequency of the corresponding linear pendulum and  $\ell$  the pendulum length, the equation of motion for a relativistic pendulum [10] readily follows:

$$\frac{d}{dt} \left( \frac{1}{\sqrt{1 - (\ell^2/c^2)(d\phi/dt)^2}} \frac{d\phi}{dt} \right) + \omega^2 \sin \phi = 0. \quad (15)$$

<sup>1</sup> If we formulated the elastic problem and its boundary conditions, unphysically, based on the ultimate deformed length  $\hat{L}$ , the information on the unique reference state would be lost, and the two problems, the elastic and relativistic, would become identical. This can be readily shown by transforming eqn (1) to  $\hat{s}$  and minimizing with respect to  $\gamma$ .

From eqn (10) we then immediately write down the explicit solution for the pendulum motion in terms of its proper time,

$$\phi(\tau) = 2 \sin^{-1} \left[ q \frac{[1 + (q\omega\ell/c)^2]^{1/2} \text{cd}(\omega\tau, m)}{[1 + (q\omega\ell/c)^2 \text{cd}^2(\omega\tau, m)]^{1/2}} \right], \quad (16)$$

where, from eqn (11),  $q = \sin(\phi_0/2)$  is related to the initial angle of the pendulum, and  $m = q^2[1 - (\omega\ell/c)^2(1 - q^2)]$ . Similarly, the proper period of the pendulum is obtained by analogy to  $\gamma_0\lambda$  of eqn (12),

$$T_\tau = 4K(m)/\omega, \quad (17)$$

and the laboratory period from  $\hat{L}/(\gamma_0 L)$  of eqn (13),

$$T_t/T_\tau = 1 + 2(\omega\ell/c)^2(1 - q^2) \left[ \frac{\Pi(q^2, m)}{K(m)} - 1 \right]. \quad (18)$$

Finally, we can transform the solution (16) to laboratory time through

$$t = \tau + \frac{2(1 - q^2)}{\omega} (\omega\ell/c)^2 [\Pi(q^2, \text{am}(\omega\tau, m), m) - \omega\tau], \quad (19)$$

In Fig. 3 we show the resulting motion of the pendulum in both proper and laboratory times. The dilation of the period of the relativistic pendulum (solid curve), compared to the nonrelativistic one (dash-dotted), illustrates the compression of the buckling wavelength in the compressible elastica compared to the incompressible case.

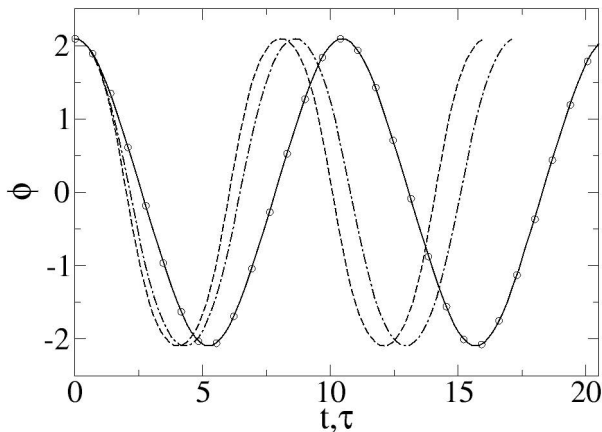


FIG. 3. Pendulum angle as a function of proper time (eqn (16), dashed line) and laboratory time (equations (16) and (19), solid line). The chosen parameters,  $\phi_0 = 2\pi/3$ ,  $\omega = 1$ ,  $(\omega\ell/c)^2 = 0.5$ , correspond to a highly relativistic pendulum resulting in a significant time dilation. Numerical solution of the equation of motion (eqn (15), circles) and the case of a nonrelativistic pendulum ( $c \rightarrow \infty$ , dash-dotted) are plotted for comparison.

We note that a similar factor to the elastic  $\gamma_0$  is encountered in certain relativistic scenarios [11, 12]. We note also that the usage of the original strain field to derive the elastic  $\gamma$  looks similar in spirit to the “einbein” used to simplify the analysis of actions in different physical contexts [13]. Unlike those analyses, however,  $\gamma$  here is an actual physical strain, the choice of which is not free but dictated by elasticity.

The extended Kirchhoff analogy presented in this Communication should be useful for studying various soft matter systems. In principle, compressibility corrections are negligible for sufficiently slender (and therefore bendable) objects. There are several indications, however, that the compressible-elastica model may be qualitatively predictive beyond its strict limits of validity. For example, it produces negative compressibility (decrease of the force  $P$  with increasing confinement) for bendability  $h^{-1}$  of order 1 [5]. Although the model is invalid for such values of  $h^{-1}$ , this result is in qualitative agreement with recent experimental and numerical results for buckled beams [14]. In ref. [4] Diggins *et al.* studied the buckling of fluid membranes under uniaxial confinement using molecular dynamics simulations. To improve the analysis of the simulation data beyond the incompressible Euler elastica, they used, on purely empirical grounds, a model which is very similar to the one presented here, obtaining good fits to the numerical results. The reason for the unexpected success of the compressible-elastica model in these two examples is unclear at present. Compressibility is essential in the case of two-dimensional deformations with non-zero Gaussian curvature. The present 1D model, as far as we know, has no applicability in such cases. It is relevant, however, to deformations with cylindrical [15, 16] or conical [17] symmetries.

We have shown above how the buckling of a compressible filament can be studied as the oscillation of a relativistic nonlinear pendulum. Here are a few suggestions for future extensions. The instability of a flat compressible rod or sheet toward curved configurations is connected to the emergence of oscillations from rest in the parametric resonance of a relativistic oscillator. A change in the compression modulus of an elastic system (e.g., as a result of a temperature change) is likened to a change in a particle’s rest mass. Lastly, the analogy can be extended to three dimensions, where the deformation of a compressible filament in 3D becomes analogous to a relativistic rotor, as outlined in Appendix A.

## ACKNOWLEDGMENTS

We thank Markus Deserno for sharing unpublished simulation results with us and for helpful discussions. This work has been supported in part by the Israel Science Foundation (Grant No. 164/14).

## Appendix A: Analogy between compressible 3D Kirchhoff's rod and relativistic rotor

In this appendix we derive the equations of equilibrium for a 3D compressible elastic rod under the assumptions of Kirchhoff's model [18, 19]. It is shown that these equations are mathematically analogous to the 3D Euler's equations of rigid-body rotation, where the non-relativistic angular momentum,  $\mathbf{L}$ , is replaced by,  $\gamma\mathbf{L}$ ,  $\gamma$  being the Lorentz factor. This analogy is derived while keeping in mind the known difficulties in the latter, relativistic problem [20, 21].

Following the formulation in ref. [22], we consider a space curve described by the position vector,  $\mathbf{R}(s)$ , where  $s$  is the arclength parameter of the relaxed configuration. Defining  $\hat{s}$  as the arclength parameter of the deformed configuration, the unit tangent vector to  $\mathbf{R}(s)$  is given by,  $\mathbf{d}_3 = d\mathbf{R}/d\hat{s}$ . In addition, let  $\{\mathbf{d}_1, \mathbf{d}_2\}$  be a pair of unit vectors perpendicular to  $\mathbf{d}_3$  and parallel to the principal axes of the filament's cross-section. The triad  $\{\mathbf{d}_1, \mathbf{d}_2, \mathbf{d}_3\}$  form a co-moving coordinate frame attached to the rod's mid-axis. These vectors satisfy the relations,

$$\frac{d\mathbf{d}_i}{ds} = \gamma\boldsymbol{\kappa} \times \mathbf{d}_i, \quad (\text{A1})$$

where  $i = 1, 2, 3$ ,  $\gamma = d\hat{s}/ds$  is the strain field, and  $\boldsymbol{\kappa} = \kappa_1\mathbf{d}_1 + \kappa_2\mathbf{d}_2 + \kappa_3\mathbf{d}_3$  is the curvature vector. The local bending moment is given by,

$$\mathbf{M}(s) = B_1(\gamma\kappa_1)\mathbf{d}_1 + B_2(\gamma\kappa_2)\mathbf{d}_2 + B_3(\gamma\kappa_3)\mathbf{d}_3, \quad (\text{A2})$$

where  $B_i$  are bending rigidities.

In correspondence with eqn (1), the energy functional of a 3D elastic filament, confined by a boundary constant

force  $\mathbf{P}$ , is given by  $E = \int_0^L e[\boldsymbol{\kappa}(s), \gamma(s)]ds$ , where

$$e[\boldsymbol{\kappa}(s), \gamma(s)] = \frac{1}{2}\mathbf{M} \cdot (\gamma\boldsymbol{\kappa}) + \frac{Y}{2}(\gamma - 1)^2 + \gamma\mathbf{d}_3 \cdot \mathbf{P}. \quad (\text{A3})$$

The appearance of the  $\gamma\boldsymbol{\kappa}$  term in the bending energy is a consequence of the requirement to keep bending and compression contributions independent. Minimizing eqn (A3) with respect to  $\gamma$  and  $\kappa_i$  (keeping in mind that  $\kappa_i$  are not independent) gives [22],

$$\frac{d\mathbf{M}}{d\hat{s}} - \mathbf{d}_3 \times \mathbf{P} = 0, \quad (\text{A4})$$

$$Y(\gamma - 1) + \mathbf{d}_3 \cdot \mathbf{P} = 0. \quad (\text{A5})$$

In the incompressible limit eqn (A5) is redundant and equations (A4) become analogous to the non-relativistic Euler equations of a 3D rigid body, fixed at one point and rotating under the influence of an external force (such as gravity) [23, p. 200]. In this analogy, the bending moment takes the role of angular momentum,  $\mathbf{M} \leftrightarrow \mathbf{L}$ , and the boundary force is analogous to an external torque,  $\mathbf{d}_3 \times \mathbf{P} \leftrightarrow \mathbf{N}$ . Turning on compressibility effects, we have by eqn (A2) that  $\mathbf{M} \rightarrow \gamma\mathbf{M}$ . Thus, it is left to show that  $\gamma$  coincides with the Lorentz factor. First integration of equations (A4) and (A5) gives,

$$\mathcal{H} = \frac{1}{2}\mathbf{M} \cdot (\gamma\boldsymbol{\kappa}) - \frac{Y}{2}(\gamma - 1)^2 - \gamma\mathbf{d}_3 \cdot \mathbf{P} = \text{const.} \quad (\text{A6})$$

Eliminating  $\mathbf{d}_3 \cdot \mathbf{P}$  from eqn (A6) and substituting in eqn (A5) gives,

$$\gamma = \frac{\sqrt{1 + 2\mathcal{H}/Y}}{\sqrt{1 + \frac{B_1}{Y}\kappa_1^2 + \frac{B_2}{Y}\kappa_2^2 + \frac{B_3}{Y}\kappa_3^2}}. \quad (\text{A7})$$

This expression indeed resembles the Lorentz factor up to the constant prefactor,  $\gamma_0 \equiv \sqrt{1 + 2\mathcal{H}/Y}$ , which appears also in the 2D problem, and which can be absorbed in the force  $\mathbf{P}$ , (see discussion in the main text).

- 
- [1] A. E. H. Love, *A Treatise on Mathematical Theory of Elasticity*, 4th edn., Dover, New York (1944).
  - [2] W. A. Oldfather, C. A. Ellis and D. M. Brown, 1933, *Isis* **20**, 72-160.
  - [3] M. Nizette and A. Goriely, *J. Math. Phys.*, 1999, **40**, 2830-2866.
  - [4] P. Diggins, Z. A. McDargh and M. Deserno, *J. Am. Chem. Soc.*, 2015, **137**, 12752-12755.
  - [5] A. Magnusson, M. Ristinmaa and C. Ljung, *Int. J. Solid Struct.*, 2001, **38**, 8441-8457.
  - [6] V. M. Vassilev, P. A. Djondjorov and I. M. Mladenov, *J. Phys. A Math. Theor.*, 2008, **41**, 435201.
  - [7] L. D. Landau and E. M. Lifshitz, *The classical theory of fields*, Butterworth-Heinemann, Oxford (1998).
  - [8] A. Humber, *Acta Mech.*, 2013, **224**, 1493-1525.
  - [9] M. Abramowitz and I. A. Stegun (eds.), *Handbook of Mathematical Functions*, Dover Publications, New York (1972).
  - [10] W. Moreau, R. Easther and R. Neutze, *Am. J. Phys.*, 1994, **62**, 531-535.
  - [11] D. Teychenné, G. Bonnaud and J. L. Bobin, *Phys. Rev. E*, 1994, **49**, 3253-5263.
  - [12] R. Anderson, I. Vetharaniam, G. E. Stedman, *Phys. Rep.*, 1998 **295**, 93-180.
  - [13] M. B. Green, J. H. Schwarz, and E. Witten, *Superstring Theory*, Vol. 1, (Cambridge University Press, 1987), Chapter 2.1.
  - [14] C. Coulais, J. T.B. Overvelde, L. A. Lubbers, K. Bertoldi, and M. van Hecke, *Phys. Rev. Lett.*, 2015, **115**, 044301.
  - [15] N. Stoop, M. M. Müller, *Int. J. Non-Linear Mech.*, 2015, **75**, 115-122.
  - [16] A. A. Lee, C. Le Gouellec, and D. Vella, *Extr. Mech.*

- Lett., 2015, **5**, 81-87.
- [17] E. Cerda, L. Mahadevan, Proc. R. Soc. A 2005 **461**, 671-700.
  - [18] E. H. Dill, Arch. Hist. Exact. Sci., 1992, **44**, 2-23.
  - [19] M. Nizette and A. Goriely, J. Math. Phys., 1999, **40**, 2830-2866.
  - [20] G. Rizzi, and M. L. Ruggiero, *Relativity in Rotating Frames*, Kluwer Academic, Dordrecht, The Netherlands (2004).
  - [21] R. Rynasiewicz, Philosophy of Science, 2000, **67**, 70-93.
  - [22] S. Lafortune, A. Goriely, M. Tabor, J. Nonlinear Dyn., 2005, **43**, 173-195.
  - [23] H. Goldstein, C. Poole, J. Safko, *Classical Mechanics*, 3rd edition, Addison-Wesley (2002).